Food Innovation and Advances

ARTICLE

Open Access

https://doi.org/10.48130/FIA-2023-0005

Food Innovation and Advances **2023**, 2(1):28–35

Effects of heat treatment on the structure, digestive property, and absorptivity of holoferritin

Ruiyang Ji, Mingyang Sun, Jiachen Zang, Chenyan Lv* and Guanghua Zhao

College of Food Science & Nutritional Engineering, China Agricultural University, Beijing Key Laboratory of Functional Food from Plant Resources, Beijing 100083, China

* Corresponding author, E-mail: 2019023@cau.edu.cn

Abstract

Ferritin, as an iron storage protein, has been considered to be a well-utilized iron supplement. However, the typical thermal processing of food rich in ferritin may affect the structure and function of ferritin as an iron supplement. Here, a plant ferritin (soybean seed ferritin, SSF) and an animal ferritin (donkey spleen ferritin, DSF) were used to analyze the changes in fundamental structure and iron content after thermal treatments (68 °C for 30 min, 100 °C for 10 min). Then, SSF and DSF after thermal treatment were administered intragastrically to mice to further evaluate its digestive stability and absorptivity after thermal processing. Results showed the secondary structure, oligomeric states, iron content, and digestive stability of DSF were maintained better than that of SSF after thermal treatments, indicating that DSF has a higher thermostability than SSF. Both SSF and DSF after thermal treatment exhibited higher absorptivity than untreated ferritins. SSF showed higher absorptivity than DSF whether heated or not.

Citation: Ji R, Sun M, Zang J, Lv C, Zhao G. 2023. Effects of heat treatment on the structure, digestive property, and absorptivity of holoferritin. *Food Innovation and Advances* 2(1):28–35 https://doi.org/10.48130/FIA-2023-0005

INTRODUCTION

Iron is an essential mineral micronutrient in life that participates in the critical metabolic progress in our body, including electron transport of the respiratory chain, oxygen transport, enzyme catalysis, and gene synthesis[1,2]. Iron deficiency is a severe nutrition deficiency problem worldwide, mainly causing iron deficiency anemia (IDA), neurodevelopment delay and even death, especially among pregnant women and children[3–5]. Iron supplements have been used for preventing iron deficiency, mainly by use of ferrous iron salts[6]. However, many reports have demonstrated ferrous iron salts have side effects or toxic effects on the body and could be easily affected by chelating agents (phytic acid, tannin) in food, leading to low bioavailability[7,8]. Therefore, it is crucial to develop an alternative iron supplement to solve the problems above.

Ferritin, an iron storage protein widely found in nature, has been considered a promising iron supplement[9,10]. Generally, the three-dimensional structure of ferritin is a well-conserved and protein shell-like structure composed of 24 subunits, with iron cores stored in the inner cavity[11,12]. And a ferritin molecule could contain up to ~4,500 Fe^{3+} atoms in the form of iron oxyhydroxide-phosphate mineral[13], which we call 'iron cores'. Ferritins from animals and plants have great variation. Animal ferritin usually consists of two types of subunits, H chain (containing a ferroxidase site) and L chain (containing a nucleation site)[11,14]. However, only one type of subunit (H chain) has been found in phytoferritin[15,16]. Besides the differences in the subunit composition, mature phytoferritin has a unique extension peptide (EP) domain on its surface, which has an iron-oxidation function and a protease activity[17,18]. What's more, the 4-fold channel of animal ferritin is hydrophobic, but that of phytoferritin is hydrophilic[19]. As a potential iron supplement, the digestive stability and absorptivity of ferritin should be addressed. Previous research demonstrated that ferritin may survive the proteolytic degradation by pepsin and pancreatic enzymes and remain intact[20]. A previous study suggested that ferritin can be mainly absorbed by the receptor-mediated endocytosis pathway[21]. Ferritin iron can also be uptaken through other pathways. If the ferritin oligomer was broken after gastrointestinal digestion, the iron cores might be reduced to ferrous iron and then uptaken by divalent metal transporter 1 (DMT1)[22,23]. Moreover, the iron cores could also remain intact for some time and be taken up by an unknown mechanism[24].

Usually, thermal treatment is a common process used during the boiling or sterilizing of food. It's important to investigate the structural and functional changes of ferritin in food under thermal treatment. As recently reported, ferritin in tofu still maintains an oligomeric state after 80 °C treatment[25]. Recently, our group has demonstrated that thermal treatment at 60–80 °C can greatly improve the storage stability of pea seeds ferritin (PSF), which may be attributed to the activity of EP[26]. However, these reports mainly focused on the plant ferritin around complex food components, thermostability of both plant and animal ferritin, and the digestive stability of ferritin *in vivo* are lacking. In this work, we aimed to evaluate the changes in fundamental structures, digestive stability and absorptivity of holoferritin, coming from both plants and animals, after thermal treatments (food processing conditions), *in vitro* and *in vivo*.

MATERIALS AND METHODS

Materials and chemicals

Soybean seeds (*Glycine max* Merr.) and donkey (*Equus* asinus) spleen were purchased from the local market (Beijing, China) and online (Hunan, China), respectively. Disodium hydrogen phosphate (Na_2HPO_4), potassium dihydrogen phosphate (KH_2PO_4), magnesium chloride ($MgCl_2$), and sodium citrate were obtained from Bio-Dee Biotechnology co. (Beijing, China). Polyvinyl pyrrolidone (PVP), sodium dodecyl sulfate (SDS), TEMED, β-mercaptoethanol, coomassie brilliant blue R-250, Native markers, and SDS markers were obtained from Sigma-Aldrich Chemical Co. (Beijing, China). Serum iron detection kit was obtained from Solarbio (Beijing, China). All of the reagents used were of analytical grade or purer.

Purification of soybean seed ferritin and donkey spleen ferritin

Soybean seed ferritin (SSF) was purified according to previous methods with a little modification[27]. Firstly, 1 kg of dry soybean seeds was soaked in distilled water overnight at 4 °C. The seeds were then blended in twice the volume of extraction buffer (50 mM Na_2HPO_4-KH_2PO_4 buffer, 1% PVP, pH 7.5) using a cooking mixer. The slurry was centrifuged at 10,000 g for 10 min at 4 °C. Subsequently, a final concentration of 0.5 M $MgCl_2$ and 0.7 M sodium citrate was added to the obtained supernatant. Then the solution was incubated for 9 h at 4 °C before centrifugation at 15,000 g for 30 min at 4 °C. The obtained brown-red pellet was resuspended in 50 mM Na_2HPO_4-KH_2PO_4 buffer (pH 7.5) and dialyzed against the same buffer, obtaining the crude protein samples. Then, the samples were applied to a DEAE-Cellulose column (ion-exchange chromatography), and ferritins were eluted with a linear gradient of sodium chloride from 0 to 1.0 M. In the end, the solution containing the ferritin was concentrated and loaded to the Superdex 75-pg gel filtration column (size-exclusion chromatography) to purify the SSF.

The donkey spleen ferritin (DSF) was purified with a similar procedure as SSF. In brief, 500 g of donkey spleen tissue was cut into small pieces and blended in an equal volume of distilled water. The slurry was centrifuged at 8,000 g for 10 min at 4 °C after filtration with a 200-mesh strainer. After adding 60% saturated ammonium sulfate to the obtained supernatant, the solution was incubated for 9 h at 4 °C. Then, the precipitant was obtained after centrifuging at 10,000 g for 30 min at 4 °C and dialyzed against 50 mM Na_2HPO_4-KH_2PO_4 buffer (pH 7.5). Last, DSF was purified by chromatography methods (ion-exchange and size-exclusion chromatography) the same as SSF. For determining the purity of ferritin, electrophoresis methods were conducted, including SDS-polyacrylamide gel (PAGE) and Native-PAGE.

Thermal treatment of the purified ferritins

The purified SSF and DSF were dialyzed against 50 mM phosphate buffer (pH 7.5) and then determined ferritin concentration according to the Bradford method with bovine serum albumin as standard. Next, the ferritins were dispensed into 1.5 mL EP tubes (0.5 mL/tube).

To investigate the effect of thermal treatment on ferritins, we chose 68 °C and 100 °C. This is due to 68 °C corresponding to the temperature of pasteurization of food, and 100 °C corresponding to high-temperature sterilization conditions during food processing. Moreover, there is a significant temperature difference between these two temperatures (68 °C is mild, and 100 °C is intense), so these two temperatures are representative to some extent and could be used for contrast. Then, ferritins (1.0 μM, 0.5 mL) were heated in a thermostatic water bath with different thermal treatments (68 °C for 10 to 30 min and 100 °C for 10 to 30 min). Finally, the protein samples after thermal treatment were centrifuged to obtain the supernatant. The supernatant of each sample was used for subsequent electrophoresis, iron content analysis, and Circular Dichroism (CD) spectra measurement to examine the structural changes of ferritins after thermal treatment.

Protein gel electrophoresis

For detecting the purity of ferritin as well as the structural changes of ferritins after thermal treatments, electrophoresis experiments were conducted. SDS-PAGE was carried out with the 15% gel. Twenty microlitres of protein sample was mixed with an equal volume of SDS loading buffer and heated in boiling water for 5 min. Subsequently, the mixture was loaded into the gel, followed by running at 150 V for 1 h. The Native-PAGE, which used 4%–20% gradient gels, was conducted to determine the native conditions of the ferritin. Twenty microlitres of protein sample was mixed with an equal volume of native loading buffer and loaded without being heated in boiling water. Then Native-PAGE was performed under conditions of 190 V for 2 h at 4 °C. The gels were later stained with Coomassie brilliant blue R-250 and captured by using the Automatic Digital Gel Image Analysis System (Tanon-2500). Gray scanning analysis of gels performed on ImageJ software showed the amount of specific protein.

Circular Dichroism (CD) spectra measurements

After the thermal treatment of ferritins, the concentration of protein samples in the supernatant was adjusted to an appropriate value (0.1 mg·mL^{-1} for SSF, 0.2 mg·mL^{-1} for DSF in pH 7.5, 50 mM phosphate buffer), with untreated ferritins as control. The far-ultraviolet (UV) CD measurements were conducted using a Pistar π-180 spectrometer (Applied Photophysics, UK) with a path length of 0.1 mm and a bandwidth of 1.0 nm. The CD data were represented by mean residual ellipticity (θ) in units of deg·cm^2·dmol^{-1}. The percentage of secondary structure was calculated using CDNN software.

Inductively Coupled Plasma Mass Spectrometry (ICP-MS) analysis

After the thermal treatment of ferritins, centrifugation was performed to isolate the supernatant. Then, we determined the concentration of the intact protein in the supernatant according to the Bradford method. Meanwhile, ICP-MS was performed to detect the iron content in the supernatant, with untreated ferritins as control. An accurate volume of 200 μL of the solution was taken from each protein sample and then 1 mL of nitric acid was added to digest for 20 min. After the digestion, the solution was diluted to 20 mL with distilled water. Finally, the iron content was detected by ICP-MS (Agilent ICPOES730, USA), and the working curve was plotted with the standard iron-containing solution. The final result of ICP-MS was presented as 'Fe/protein shell' in the supernatant.

Animal study

An animal experiment was conducted to evaluate the effect of thermal treatment on digestion stability and iron

bioavailability of ferritins. Four-week-old, healthy male KM mice with a balanced initial body weight of 30 ± 5 g were purchased from Beijing Vital River Laboratory Animal Technology Co., Ltd. (China). Mice were acclimatized for 3 d in appropriate conditions (a temperature of 25 ± 2 °C, a 12 h light/dark cycle, humidity at 55% ± 5%, with distilled deionized water and food continuously given). The following animal experiments were conducted in strict accordance with the guidelines for the care and use of laboratory animals of the Animal Welfare and Animal Experiment Ethics Review Committee of China Agricultural University (CAU), with permission number AW82402202-4-1.

Twenty-one mice were randomly assigned into seven groups (n = 3), including one blank control groups, three SSF-treated groups (administering SSF of untreated, 68 °C for 30 min and 100 °C for 10 min, respectively), and three DSF-treated groups (administering DSF of untreated, 68 °C for 30 min and 100 °C for 10 min, respectively), and transferred to stainless steel cages. Before intragastric administration, mice fasted overnight. Mice in the blank control group were administered with 300 μL of 10 mM phosphate buffer (pH 7.5). In experimental groups, the purified SSF and DSF with different thermal treatments were administered intragastrically to mice, with untreated ferritins as control. The specific steps of ferritins were administered as follows: firstly, the purified SSF and DSF were dialyzed against 10 mM phosphate buffer (pH 7.5). Secondly, the concentration of SSF and DSF was adjusted to about 2.4 mg·mL^{-1} and 1.5 mg·mL^{-1}, respectively, both equivalent to an iron dose of 5.0 mg·kg^{-1} mouse weight. Then, SSF and DSF samples were all heated at 68 °C for 30 min and 100 °C for 10 min. The samples without thermal treatment were used as a control. Lastly, 300 μL of the total heat-treated ferritins without removing the precipitation or untreated ferritin sample were administered to each mouse in the group.

As reported, the time for ferritin to reach the intestine is about 1–2 h[13]. Thus, 1 h after the intragastric administration, blood samples (about 0.4 mL) were collected from eye ground vein into heparinized microcentrifuge tubes and stored at −20 °C until analysis, and mice were sacrificed by cervical dislocation. The small intestine tissues were subsequently removed rapidly from mice and placed on ice. The content of small intestine tissues were collected by squeezing the tissue with forceps and immediately stored at the −20 °C. Next, Native-PAGE was further conducted to detect the digested ferritins in small intestinal contents. The intestinal content of one mouse in each group was mixed with 20 μL of 10 mM phosphate buffer (pH 7.5) and 20 μL of Native loading buffer. After stirring and centrifuging the mixture to discard residue, the Native-PAGE using 4%–20% gradient gel was conducted to detect the supernatant under conditions of 190 V for 2 h at 4 °C.

Serum iron content measurements

The serum was separated by centrifuging the blood samples at 4,000 g for 10 min. The serum iron content was measured using the multifunctional enzyme marker (Varioskan Flash, USA), following the procedures of serum iron detection kit.

Statistical analysis

Experiments were conducted in triplicates. Data values are expressed as means ± standard deviation (SD). Statistical analyses were estimated with SPSS 25.0 software. The data were determined by one-way analysis of variances (ANOVA), and the differences were significant when $P < 0.05$.

RESULTS

Structural changes of SSF and DSF after thermal treatment

SSF and DSF were isolated and purified from soybean seeds and donkey spleen tissue, respectively. As shown in Fig. 1a, both native SSF and DSF were composed of two types of subunits, H-1 (26.5 kDa, lower band) and H-2 (28.0 kDa, upper band) of SSF, L (around 19.0 kDa, lower band) and H (around 21.0 kDa, upper band) of DSF. While, as shown in Fig. 1b, there is almost only one band for both purified SSF and DSF, which are the same as that of other typical plant and animal ferritins composed of 24 subunits[11,14].

To illustrate the effects of the thermal process on ferritins, the subunit and oligomeric states of ferritins after thermal treatment (68 °C from 10 to 30 min; 100 °C from 10 to 30 min) were identified. As shown in Fig. 2, it appeared that the subunit compositions of both SSF (Fig. 2a) and DSF (Fig. 2b) were basically not degraded upon thermal treatment. The Native-PAGE of SSF was shown in Fig. 2c, untreated SSF maintained an individual ferritin molecule (560 kDa). According to the gray-scale analysis, there was 14%–16% denaturation of SSF upon 68 °C thermal treatments from 10 to 30 min, whereas 100 °C heated from 10 to 30 min caused most of the SSF (80%–98%) to be denatured by dissociating into smaller subunits. Interestingly, DSF molecules were mostly kept stable even at 100 °C for 10 min (Fig. 2d). These results indicated that the thermostability of SSF and DSF was different, because the shell-like structure of SSF was almost destroyed upon high temperature sterilization, whereas most of the shell-like structure of DSF remained intact. However, the status of iron cores inside the ferritin remains to be determined.

Based on the results above, thermal conditions with 68 °C for 30 min and 100 °C for 10 min were selected to treat SSF and DSF for further study. To figure out the effect of thermal treatment on the secondary structure of SSF and DSF, the CD spectra of thermal treated SSF and DSF were further conducted with untreated ferritins as control (Fig. 3). In Fig. 3a, the CD spectrum of untreated SSF had the typical characteristics of α-helical ferritins with negative ellipticity at 207 nm and 222 nm in the far-ultraviolet (UV) spectrum, which is in agreement with a previous report of native SSF structure[28]. And the composition of secondary structure of untreated SSF were 59% of α-helix and 21% of random coil. However, the CD spectrum of SSF heated at 68 °C for 30 min and 100 °C for 10 min showed a

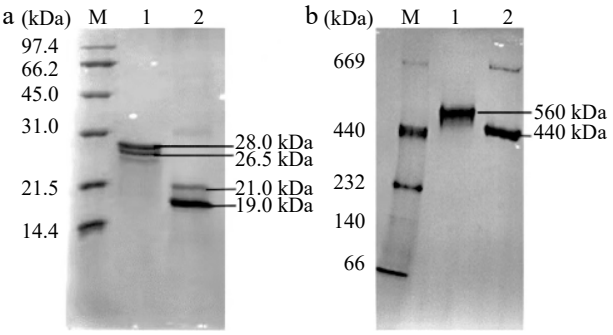

Fig. 1 Electrophoresis analyses of 1.0 μM of SSF and DSF. (a) SDS-PAGE analysis. (b) Native-PAGE analysis. Lane 1: SSF; Lane 2: DSF; Lane M: Protein markers.

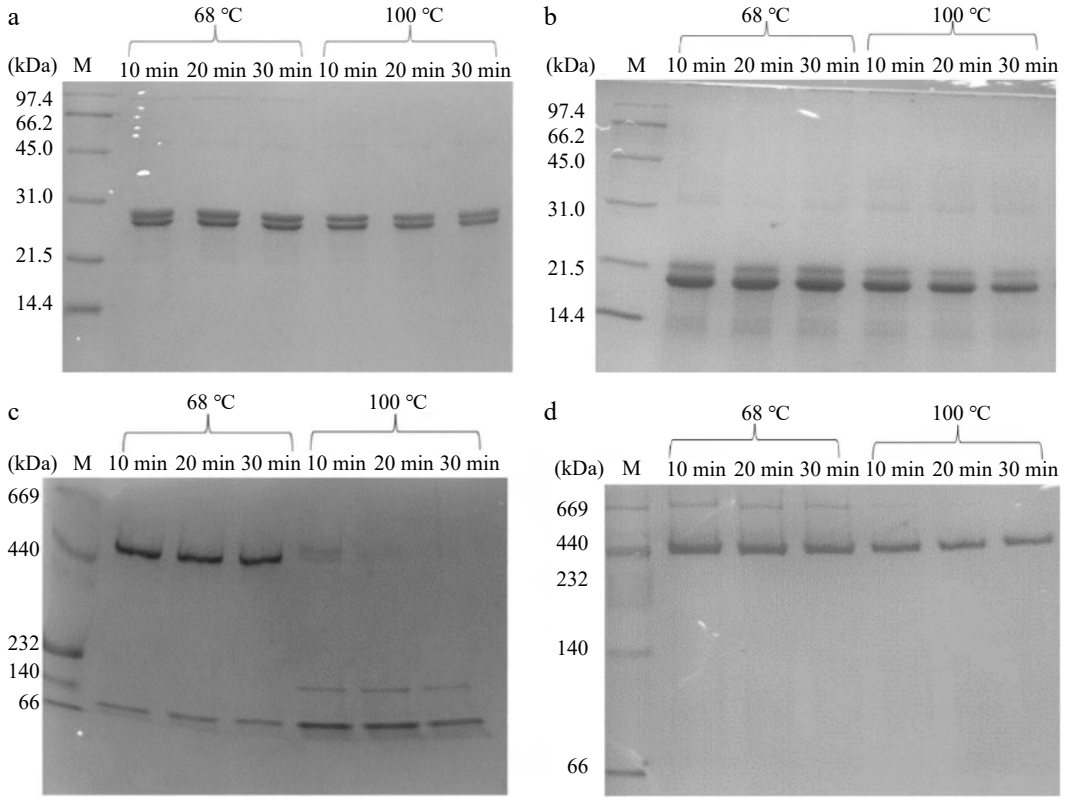

Fig. 2 Electrophoresis analyses of 1.0 μM of SSF and DSF after different thermal treatments. (a) SDS-PAGE analysis of SSF. (b) SDS-PAGE analysis of DSF. (c) Native-PAGE analysis of SSF. (d) Native-PAGE analysis of DSF. Lane M: Protein markers.

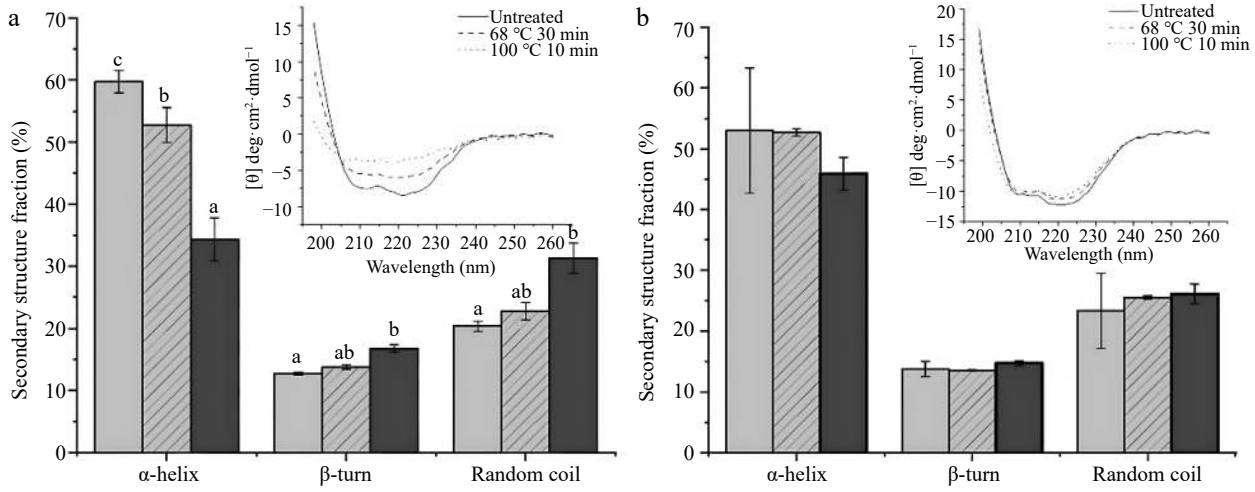

Fig. 3 CD spectra results of ferritins under conditions of untreated, 68 °C for 30 min and 100 °C for 10 min. (a) CD spectra and percentages of the secondary structure of 0.1 mg/mL SSF. (b) CD spectra and percentages of the secondary structure of 0.2 mg·mL^{-1} DSF. Values are means ± SD, and different letters in the column indicate significant difference ($P < 0.05$) between treatments.

noticeable difference. In detail, the typical α-helix curves of SSF greatly changed, and the mean percentages of α-helix decreased to 52% and 34% respectively, whereas random coil increased to 22% and 31% respectively. These spectral results of SSF indicated the secondary structure of SSF was affected after the thermal process, especially at 100 °C for 10 min.

In contrast, the secondary structures of DSF were kept unchanged under the same thermal treatments as SSF. As shown in Fig. 3b, the typical α-helix spectral curves of DSF were identical whether heated or not. And compared with untreated DSF, the ratio of α-helix of DSF treated with 68 °C for 30 min and 100 °C for 10 min decreased slightly from 53% to 52% and 46% respectively. There is no significant difference between them ($P > 0.05$). These results showed thermal treatments have no significant effect on the secondary structure of DSF, suggesting the structure of DSF was more stable than SSF, which is in accordance with the native-PAGE result.

Effect of thermal treatments on the iron content of SSF and DSF

During thermal processing, the iron release is always along with the denaturation of ferritin[26]. Thus, it is crucial to further determine the changes in iron content of ferritin during the thermal process. To explore the case of iron release after thermal treatment, the iron content of SSF and DSF after thermal treatments were analyzed. In Fig. 4a, it was found that the iron content of SSF treated with 68 °C, 30 min (1,056 ± 136 iron/protein shell) and 100 °C, 10 min (696 ± 62 iron/protein shell) are much lower than that of the native SSF (2,133 ± 152 iron/protein shell). Moreover, there was also a significant difference between the iron content of SSF heated at 68 °C for 30 min and 100 °C for 10 min ($P < 0.05$). SSF treated with high temperature releases iron much more easily. These results indicated more than half of the iron in SSF was released from the protein shell during the thermal process, which might be related to the changes in the tertiary and secondary structure of SSF after thermal treatments (Fig. 2c, 3a).

Similarly, small portions of iron also released from DSF during the thermal treatments (Fig. 4b). Specifically, the iron content of DSF without thermal treatment was 2,110 ± 152 iron/protein shell, while the iron content of DSF decreased to 1,547 ± 14 iron/protein shell (68 °C for 30 min) and 1,390 ± 71 iron/protein shell (100 °C for 10 min), respectively. By comparing the iron content of DSF with that of SSF after thermal treatment, iron content in DSF is 50% higher than that in SSF, which might be due to the high stability of DSF after thermal treatment.

Effect of thermal treatments on *in vivo* digestive stability of SSF and DSF

Since ferritin has been considered a well-utilized source of dietary iron, it is essential to assess the effects of thermal treatments during food processing on its digestive stability *in vivo*. SSF and DSF samples after thermal treatment were used without centrifugation to remove denatured proteins and iron core. Firstly, after intragastric administration of SSF and DSF samples for 1 h, the intestinal contents of mice were collected, and the composition of intestinal contents was identified by Native-PAGE. We have used the intestine content of mice administered with equal volume of PBS as the control. As seen in Fig. 5, one SSF band was detected in the intestine of mice administered with untreated SSF (lane 1), whereas the bands corresponding to SSF heated at 68 °C for 30 min and 100 °C for 10 min (lanes 2 and 3) were not detectable. These results indicated that thermal treatments on SSF greatly affected the digestive stability of SSF *in vivo*. In contrast, the bands corresponding to untreated DSF, DSF treated at 68 °C for 30 min, and DSF treated at 100 °C for 10 min (lanes 4–6) were detectable by Native-PAGE, suggesting thermal treatments had no apparent influence on the digestive stability of DSF.

Effect of thermal treatments on the iron bioavailability of SSF and DSF

In order to evaluate the effect of thermal treatments on the bioavailability of ferritin iron *in vivo*, the serum iron content were analyzed after administration of SSF and DSF. To guarantee the identical dosage of iron administered, ferritin samples after heat treatment were given to the mice without removing the released iron core and denatured protein molecules. As shown in Fig. 6, the serum iron content of untreated SSF group was 50 ± 8 μM, and that of SSF heated at 68 °C for 30 min and 100 °C for 10 min are 52 ± 19 μM and 56 ± 13 μM, respectively, showing the significant increase of iron bioavailability after thermal treatments ($P < 0.05$). This result is in accordance with previous results that thermal processing can improve the iron uptake at Caco-2 cell[29]. However, the serum iron content of DSF were 40 ± 11 μM for untreated, 45 ± 15 μM for DSF heated at 68 °C for 30 min and 44 ± 10 μM for DSF heated at 100 °C for 10 min and there is no significant difference among them.

DISCUSSION

Ferritin is ubiquitous in living kingdoms and has recently been developed as a novel iron supplement. However, in foodstuff, ferritin must bear various kinds of treatments such as heat and light. Although previous research has suggested the heat-stable property of ferritin, ferritins from different sources may show differences in their properties. In this research, we chose DSF from animal sources and SSF from plant sources to find out the differences in their thermostability, digestive stability and absorptivity.

We first assessed the effect of thermal treatments on the essential structures of ferritin. The results showed most of the SSF was denatured after thermal treatment (Fig. 2c), along with

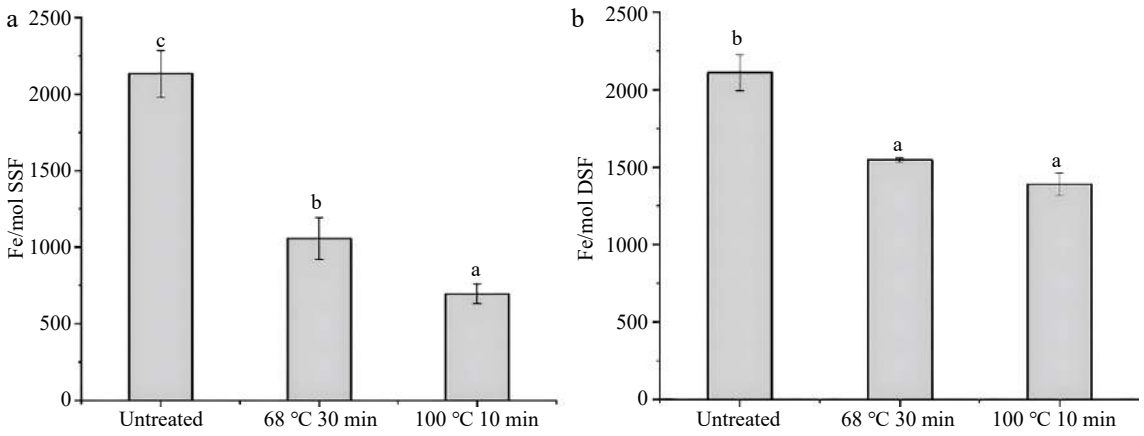

Fig. 4 Iron content of ferritins after thermal treatment measured by ICP-MS, with untreated as a control. (a) and (b) are the iron content of SSF (1.0 μM) and DSF (1.0 μM) under conditions of untreated, 68 °C for 30 min and 100 °C for 10 min, respectively. Values are means ± SD, and different letters in the column indicate significant differences ($P < 0.05$) between treatments.

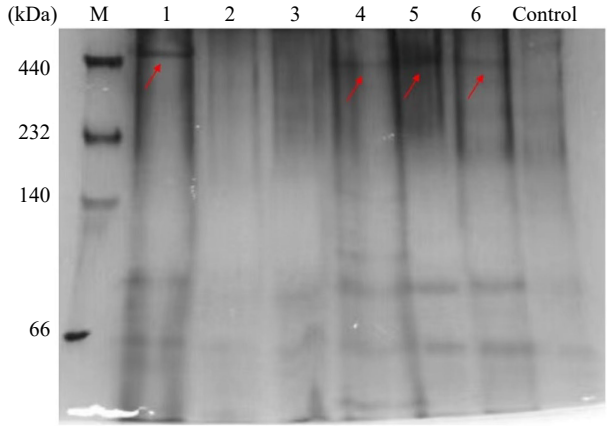

Fig. 5 *In vivo* digestion results of SSF and DSF after different treatments. Lanes 1–3: Untreated, 68 °C for 30 min, 100 °C for 10 min of SSF; Lanes 4–6: Untreated, 68 °C for 30 min, 100 °C for 10 min of DSF. Control group: mice administered with 300 μL of 10 mM phosphate buffer. The electrophoresis was performed three times, with similar results obtained.

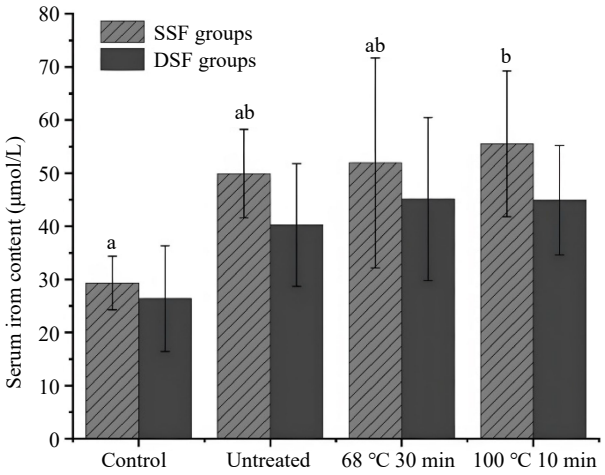

Fig. 6 Serum iron content of mice in SSF groups and DSF groups. The letters indicate inner group comparisons of SSF groups ($P < 0.05$). There is no statistical difference of DSF groups ($P > 0.05$). Control group: mice administered with 300 μL of 10 mM phosphate buffer. Values are means ± SD, and different letters in the column indicate significant differences ($P < 0.05$) between treatments.

the majority of iron being released (Fig. 4a). In contrast, DSF remined stable after thermal treatment, and little iron was released from the protein shell (Fig. 2d, 4b). These results showed that SSF is not as stable as DSF after thermal treatment, the reason for which can be attributed to the subunit compositions, and need further investigation. Based on previous reports, the unique EP domain of SSF is sensitive to thermal temperature during thermal processing[17,26,30]. We speculate that the degradation of EP induced by thermal treatment destabilizes the protein structure and causes the difference of thermostability between SSF and DSF. Besides, as reported, there are other structural factors affecting the thermostability of ferritins, such as salt bridges and hydrogen bonds[31,32]. For instance, a previous report suggested that the amino acid residues around three-fold channels contribute to the high thermostability of shrimp ferritin[30]. The differences in amino acids around four-fold channels (Supplemental Fig. S1) may also contribute to the thermostability, which needs further investigation. Thus, there may be complex factors resulting in the difference in the thermostability, including the amino acid residues and so on.

The form and content of iron in ferritin after thermal treatment are highly related to the iron bioavailability of ferritin. Not surprisingly, the iron content of ferritins after thermal treatment were much lower than that of ferritin without treatment. In accordance with the thermostability of ferritin, iron content of DSF is much higher than that of SSF especially after being heated at 100 °C for 10 min, indicating iron released from DSF is little and only small a part of DSF was denatured. That can be explained by the high thermostability of DSF, the fold channels which are responsible for iron release have not been destroyed during thermal treatment[19] and a large amount of iron remained inside the DSF protein shell.

As a promising dietary iron supplement, the changes in digestive stability and absorptivity of ferritin after thermal treatments were further determined. In terms of the digestive situation (Fig. 5), the differences in digestive stability of SSF and DSF can be attributed to the stability of SSF and DSF after thermal treatment. SSF which is partially denatured after thermal treatment was much easier to be digested by proteases in the gastrointestinal tract[28,33]. After partially denaturation, much more enzymatic sites of SSF are exposed to the proteases such as pepsin and trypsin[26].

As an iron supplement, whether ferritin iron can be absorbed efficiently is notable to determine. As for absorptivity, we can find that the serum iron content of all SSF and DSF groups were higher than that of control groups (Fig. 6), suggesting iron associated with the ferritins with and without thermal treatment could be absorbed by mice. And importantly, the absorptivity of SSF and DSF after thermal treatment was higher than that of ferritins without thermal treatment. The reason for higher absorptivity can be attributed to the iron forms in ferritin after thermal treatment. As previously reported, part of iron released from ferritin. To keep the amount of iron administered by mice the same, we use ferritins without removing the precipitate. That means iron core, free iron and iron within the ferritin shell coexist in ferritin samples before intragastric administration. Combined with the changes in iron content upon thermal treatment of SSF and DSF (Fig. 4), we speculate that the ferritins with released iron after thermal treatment were more easily absorbed than the intact, untreated ferritins. This speculation was further confirmed by the results of DSF. DSF with high thermal stability and digestive stability showed lower iron bioavailability *in vivo* than SSF, which might be explained as follows: firstly, there were larger portions of iron cores released from SSF than that from DSF during the thermal process; secondly, a large amount of intact protein-shell structure of DSF existed after digestion, whereas SSF didn't (Fig. 5); lastly, different subunit compositions of ferritins (Supplemental Fig. S1) may have different affinities with its potential receptor in the intestine such as Transferrin Receptor 1 (TfR1), causing different absorbing efficiency[13].

Recently, possible intestinal absorption pathways of ferritin have been extensively studied. We propose that a large part of untreated SSF and DSF could escape digestive degradation and be directly absorbed into enterocytes through some specific receptors, such as TfR1, Scara 5, and assembly peptide 2

(AP2)[34–36]. At the same time, the released iron cores of SSF and DSF after thermal treatment might be entirely absorbed by endocytosis or might translate to iron ions and then taken up by the DMT1 receptor[24,37]. Based on the results obtained from the animal experiment, we believe the pathway of iron cores plays a principal role in iron absorption among three pathways. Thus, we can conclude that iron from DSF with high thermal stability are mainly absorbed in the form of intact ferritin in the intestine, whereas iron from SSF, which may be denatured during food processing and degraded during digestion, are mainly absorbed in the form of released iron and ferritin associated iron. Iron bioavailability from released iron is much higher than that from ferritin molecules. In the future, it's deserved to focus on the form of released iron (free iron or iron cores) and the possible absorption mechanism.

CONCLUSIONS

In the present study, we illustrated the changes in subunit compositions, the oligomeric states, the secondary structure, and the iron contents of SSF and DSF during the thermal process. And combining with the structural changes above, we found the thermostability and the digestive stability of SSF is much lower than that of DSF, which may be related to the difference in subunit compositions and structures. Moreover, the iron bioavailability of SSF was higher than DSF, from which we propose iron cores pathway has a higher efficiency than the receptor-mediated endocytosis pathway for intact ferritin, whereas the detailed mechanism needs to be explored. Thus, phytoferritin has a promising application as an iron supplement, especially in vegetarian and meat-scarce countries. Therefore, thermal treatments during the processing of food rich in ferritins may promote its absorptivity, providing a theoretical guidance for the thermal process of ferritin as an iron supplement.

ACKNOWLEDGMENTS

This research was funded by National Natural Science Foundation of China (No. 31730069).

Conflict of interest

The authors declare that they have no conflict of interest.

Supplementary Information accompanies this paper at (https://www.maxapress.com/article/doi/10.48130/FIA-2023-0005)

Dates

Received 23 November 2022; Accepted 19 January 2023; Published online 2 March 2023

REFERENCES

1. Vogt ACS, Arsiwala T, Mohsen M, Vogel M, Manolova V, et al. 2021. On iron metabolism and its regulation. *International Journal of Molecular Sciences* 22(9):4591
2. Abbaspour N, Hurrell R, Kelishadi R. 2014. Review on iron and its importance for human health. *Journal of Research in Medical Sciences* 19(2):164–74
3. Georgieff MK. 2020. Iron deficiency in pregnancy. *American Journal of Obstetrics and Gynecology* 223(4):516–24
4. Camaschella C. 2019. Iron deficiency. *Blood* 133(1):30–39
5. Benson CS, Shah A, Stanworth SJ, Frise CJ, Spiby H, et al. 2021. The effect of iron deficiency and anaemia on women's health. *Anaesthesia* 76(S4):84–95
6. Auerbach M, Adamson JW. 2016. How we diagnose and treat iron deficiency anemia. *American Journal of Hematology* 91(1):31–38
7. Muñoz M, Gómez-Ramírez S, Bhandari S. 2018. The safety of available treatment options for iron-deficiency *Anemia*. *Expert Opinion on Drug Safety* 17(2):149–59
8. Tolkien Z, Stecher L, Mander AP, Pereira DIA, Powell JJ. 2015. Ferrous sulfate supplementation causes significant gastrointestinal side-effects in adults: a systematic review and meta-analysis. *Plos One* 10(2):e0117383
9. Zhang C, Zhang X, Zhao G. 2020. Ferritin nanocage: a versatile nanocarrier utilized in the field of food, nutrition, and medicine. *Nanomaterials* 10(9):1894
10. Huang Y, Xin M, Li Q, Luo X, Wang X, et al. 2014. Chickpea seeds ferritin as a potential source in the treatment of iron deficiency anemia. *Journal of Food and Nutrition Research* 2(12):876–79
11. Harrison PM, Arosio P. 1996. The ferritins: molecular properties, iron storage function and cellular regulation. *Biochimica et Biophysica Acta (BBA) - Bioenergetics* 1275(3):161–203
12. Liu Y, Yang R, Liu J, Meng D, Zhou Z, et al. 2019. Fabrication, structure, and function evaluation of the ferritin based nanocarrier for food bioactive compounds. *Food Chemistry* 299:125097
13. Lv C, Zhao G, Lönnerdal B. 2015. Bioavailability of iron from plant and animal ferritins. *J Nutr Biochem* 26(5):532–40
14. Stefanini S, Cavallo S, Wang CQ, Tataseo P, Vecchini P, et al. 1996. Thermal stability of horse spleen apoferritin and human recombinant H apoferritin. *Archives of Biochemistry and Biophysics* 325(1):58–64
15. Li C, Hu X, Zhao G. 2009. Two different H-type subunits from pea seed (pisum sativum) ferritin that are responsible for fast Fe(II) oxidation. *Biochimie* 91(2):230–39
16. Liao X, Yun S, Zhao G. 2014. Structure, function, and nutrition of phytoferritin: a newly functional factor for iron supplement. *Critical Reviews in Food Science and Nutrition* 54(10):1342–52
17. Fu X, Deng J, Yang H, Masuda T, Goto F, et al. 2010. A novel EP-involved pathway for iron release from soya bean seed ferritin. *The Biochemical Journal* 427:313–21
18. Yang H, Fu X, Li M, Leng X, Chen B, et al. 2010. Protein association and dissociation regulated by extension peptide: a mode for iron control by phytoferritin in seeds. *Plant Physiology* 154(3):1481–91
19. Lv C, Zhang S, Zang J, Zhao G, Xu C. 2014. Four-fold channels are involved in iron diffusion into the inner cavity of plant ferritin. *Biochemistry* 53(14):2232–41
20. Bejjani S, Pullakhandam R, Punjal R, Nair KM. 2007. Gastric digestion of pea ferritin and modulation of its iron bioavailability by ascorbic and phytic acids in caco-2 cells. *World Journal of Gastroenterology* 13(14):2083–88
21. Kalgaonkar S, Lönnerdal B. 2009. Receptor-mediated uptake of ferritin-bound iron by human intestinal Caco-2 cells. *The Journal of Nutritional Biochemistry* 20(4):304–11
22. Anderson GJ, Frazer DM. 2017. Current understanding of iron homeostasis. *The American Journal of Clinical Nutrition* 106:1559S–1566S
23. Yanatori I, Kishi F. 2019. DMT1 and iron transport. *Free Radical Biology & Medicine* 133:55–63
24. Lönnerdal B. 2009. Soybean ferritin: implications for iron status of vegetarians. *The American Journal of Clinical Nutrition* 89:S1680–S1685
25. Masuda T. 2015. Soybean ferritin forms an iron-containing oligomer in tofu even after heat treatment. *Journal of Agricultural and Food Chemistry* 63(40):8890–95

26. Tang J, Yu Y, Chen H, Zhao G. 2019. Thermal treatment greatly improves storage stability and monodispersity of pea seed ferritin. *Journal of Food Science* 84(5):1188–93
27. Deng J, Cheng J, Liao X, Zhang T, Leng X, et al. 2010. Comparative study on iron release from soybean (*Glycine max*) seed ferritin induced by anthocyanins and ascorbate. *Journal of Agricultural and Food Chemistry* 58(1):635–41
28. Deng J, Li M, Zhang T, Chen B, Leng X, et al. 2011. Binding of proanthocyanidins to soybean (*Glycine max*) seed ferritin inhibiting protein degradation by protease in vitro. *Food Research International* 44(1):33–38
29. Xing Y, Ma J, Yao Q, Chen X, Zang J, et al. 2022. The Change in the Structure and Functionality of Ferritin during the Production of Pea Seed Milk. *Foods* 11:557
30. Zhang X, Zang J, Chen H, Zhou K, Zhang T, et al. 2019. Thermostability of protein nanocages: the effect of natural extra peptide on the exterior surface. *RSC Advances* 9(43):24777–82
31. Tan X, Liu Y, Zang J, Zhang T, Zhao G. 2021. Hyperthermostability of prawn ferritin nanocage facilitates its application as a robust nanovehicle for nutraceuticals. *International Journal of Biological Macromolecules* 191:152–60
32. Tatur J, Hagen WR, Matias PM. 2007. Crystal structure of the ferritin from the hyperthermophilic archaeal anaerobe *Pyrococcus furiosus*. *Journal of Biological Inorganic Chemistry* 12:615–30
33. Hoppler M, Schönbächler A, Meile L, Hurrell RF, Walczyk T. 2008. Ferritin-iron is released during boiling and in vitro gastric digestion. *The Journal of Nutrition* 138(5):878–84
34. Lönnerdal B, Bryant A, Liu X, Theil EC. 2006. Iron absorption from soybean ferritin in nonanemic women. *The American Journal of Clinical Nutrition* 83(1):103–7
35. Martin CDS, Garri C, Pizarro F, Walter T, Theil EC, et al. 2008. Caco-2 intestinal epithelial cells absorb soybean ferritin by μ_2 (AP2)-dependent endocytosis. *The Journal of Nutrition* 138(4):659–66
36. Yu B, Cheng C, Wu Y, Guo L, Kong D, et al. 2020. Interactions of ferritin with scavenger receptor class A members. *The Journal of Biological Chemistry* 295(46):15727–41
37. Kalgaonkar S, Lonnerdal B. 2008. Effects of dietary factors on iron uptake from ferritin by Caco-2 cells. *The Journal of Nutritional Biochemistry* 19(1):33–39